ACS OMEGA

http://pubs.acs.org/journal/acsodf

Article

Simulation of Biomass Air Gasification in a Bubbling Fluidized Bed Using Aspen Plus: A Comprehensive Model Including Tar Production

Maryem Dhrioua, Kaouther Ghachem, Walid Hassen,* Ahmed Ghazy, Lioua Kolsi, and Mohamed Naceur Borjini

Cite This: *ACS Omega* 2022, 7, 33518−33529

Read Online

ACCESS | Metrics & More | Article Recommendations

ABSTRACT: This work studied a multistage gasification system that is designed for producing a syngas with a low tar content. The proposed system is an atmospheric bubbling fluidized-bed gasifier and comprises mainly pyrolysis, combustion, and gasification zones. The numerical investigation is performed using Aspen Plus to study Prosopis Juliflora gasification. Chemical reactions as well as tar treatment in the process are investigated. Two different pyrolysis temperatures were considered: 500 and 600 °C, along with three different particle size ranges: 0.2−0.5, 0.5−1, and 1−2 mm. The effect of the air-to-biomass ratio, with values from 0.2 to 1.2, and the gasification reactor temperature, from 800 to 1000 °C, on the composition of product gas and tar species formation during the process (phenol, naphthalene, benzene, and toluene), its lower heating value (LHV), and cold gasification efficiency (CGE) were studied. Results showed that a pyrolysis temperature of 600 °C and a particle size range of 0.2−0.5 mm displayed less tar produced from both combustion and gasification zones and were associated with greater CO, H_2, and CH_4 yields, compared to the other pyrolysis parameters tested. Increasing the gasification temperature led to increasing the CO, H_2, and tar yields and decreasing the CH_4 yield and CGE. The maximum CGE combined with the minimum tar amount produced could be obtained with values of 800 °C and 1.2 for the gasification temperature and the air-to-biomass ratio, respectively. The numerical simulation results will be used to improve the performance of the proposed system.

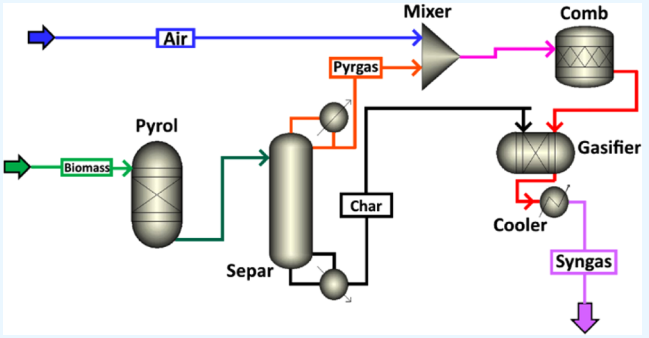

INTRODUCTION

Biomass gasification is a thermochemical process that uses heat to transform biomass into a producer syngas through sequences of homogeneous and heterogeneous chemical reactions. This gas typically contains CO, H_2, CH_4, N_2, and other components such as CO_2 and tar that are undesirable. Biomass gasification is widely used for heat and power generation.[1]

During the process, both heat and mass transfers are implicated. The biomass gasification process includes three processes: pyrolysis, combustion, and reduction. Several works have studied the impact of significant factors on the producer gas composition and impurities. Fluidized-bed processes are generally used to improve the contact between gas and solid particles and, thus, to endorse the conversion of biomass feedstock. Additionally, they can operate effectively with a wide range of biomasses. Multistage gasification systems are also recommended to promote the quality of the product gas by reducing its tar content.[2−10] This could be done using char in the fluidized bed. Regarding pyrolysis, it consists of a set of tremendously complex reactions. However, several works[11,12] assumed pyrolysis as an instantaneous process. In fact, it is almost accomplished at the feed inlet of the gasifier. Conferring to these assumptions, the pyrolysis product composition can be used as an input in gasification models. Besides, it is a practical methodology to simplify complicated biomass gasification models. For this purpose, empirical correlations based on experimental data for pyrolysis were used.[13−16] Further common description of biomass pyrolysis products can be found in Neves et al.'s work.[17]

In recent years, numerous researchers have focused their attention on modeling biomass gasification using Aspen Plus,[18−21] which is a process software that is used to model energy and mass balance equations in multiphase models. Niu et al.[22] established a comprehensive Aspen Plus model inside a fluidized-bed gasifier designated to simulate municipal solid waste gasification. The authors specified that the H_2 and CO production as well as the gasification efficiency were improved

Received: July 16, 2022
Accepted: August 26, 2022
Published: September 2, 2022

with the increase of the temperature. Analogous results were established by Beheshti et al.,[13] which was developed in the Aspen Plus process model for air-steam biomass gasification inside a bubbling fluidized bed. The authors showed that the equivalence ratio was the main factor in the system. In fact, higher values of the equivalence ratio caused larger syngas production, carbon conversion, and tar reforming. Mitta et al.[23] studied a model for a fluidized-bed-type gasification process under several conditions. They varied the flow rate, the operating pressure and temperature, and the composition and temperature of the feeding material. The established model was appropriate to evaluate the syngas composition along with the influence of operating temperature.

Renganathan et al.[24] stated that the stoichiometric or nonstoichiometric method can be used to model gasification of a carbonaceous feedstock. The stoichiometric method specifies a series of reactions. A selection of species expected in the syngas is defined in the nonstoichiometric method. Besides, information about these reactions is not needed. As a result, the Gibbs minimization technique is more general and can be used in accordance with multiphase equilibriums. Puigarnavat et al.[18] stated that the applicability of kinetic rate models to various plants is often limited. Additionally, conducting process studies that focus on the effect of the most critical system parameters may be better served by thermodynamic equilibrium calculations. A reacting system has a stable composition and is considered at chemical equilibrium when the generated entropy is maximum and the Gibbs free energy is minimum. Models based on thermodynamic equilibrium have been commonly used as they showed reasonable agreement with experimental results.[18] In Aspen Plus, the RGIBBS block is a module based on the Gibbs minimization methodology. It is employed to model gasification systems thermodynamically. Ravikiran et al.[25,26] explained the usage of the Gibbs equilibrium approach to model a gasifier. Niu et al.[22] used the RGIBBS block to model both partial oxidation and gasification sections to simulate gasification in a bubbling fluidized bed using Aspen Plus. Doherty et al.[20] studied a circulating fluidized-bed gasifier using Aspen Plus with the Gibbs free energy minimization, and a good concurrence with experimental data showed that the model predicted well the syngas composition, conversion efficiency, and heating values.

From the previously cited studies, we can conclude that equilibrium-based models can be efficiently used for simulating fluidized-bed gasifiers. However, most of them did not consider tar or considered it as chemically inert. Tar is a highly undesirable viscous liquid that can eventually condense in a gasifier's low-temperature areas, clogging the flow of gas and causing system disruption. Nonetheless, it is an inescapable byproduct of thermal conversion, and accordingly, numerous recent models focused on its modeling. Su et al.[27] studied experimentally the tar destruction in a continuous reactor system under an environment of biomass partial oxidation. Results showed that tar amounts decreased rapidly with the equivalence ratio. This resulted in an increase in the total gas volume. According to the authors, aromatics are the most prevailing species in tertiary tar, such as naphthalene, fluorene, phenanthrene, and pyrene. Su et al.[27] studied tar decomposition numerically and compared it to experimental data. The considered tar components were phenol, toluene, benzene, and naphthalene. A good qualitative agreement was obtained. This decreasing behavior of tar amount produced as a function of the equivalence ratio (ER) was also mentioned by Beheshti et al.[13] Thus, to reduce tar formation, it was essential to operate the gasification process at higher equivalence ratios. Additionally, the tar concentration increased if the biomass particle size decreased.[13] Abdelouahed et al.[14] proposed an Aspen Plus model for a dual fluidized-bed gasifier. Ten tar species grouped in four tar model compounds. They were provided by a correlation. The authors concluded that different dual fluidized-bed reactor designs could be modeled with Aspen Plus to optimize the tar destruction zone. Kaushal et al.[28] used Aspen Plus to develop a model for biomass gasification in a bubbling fluidized gasifier. A submodel for tar production and cracking was incorporated in this model. The results showed that the gasification process was enhanced for higher temperatures. Also, the hydrogen production was increased, and the tar content was diminished. Liu et al.[29] performed experiments using rice straw in a two-stage fluidized bed. It was shown that the temperature enhances the gasification performance. However, increasing the ER had a negative effect on the gas heating value. Masmoudi et al.[30] investigated experimentally and numerically the gasification of almond shells. They considered a downdraft gasifier and focused on the partial oxidation and thermal cracking of tar. The interaction between the homogeneous and heterogeneous chemical reactions was included in their model. The authors analyzed the performance of the gasifier with regard to the product gas composition and tar conversion. To model tar treatment, six species were taken into consideration: phenol, toluene, benzene, naphthalene, hydroxy-acetaldehyde, and hydroxy-acetone. The authors concluded that the total tar conversion reached 93%. They affirmed that the modeling approach could be considered appropriate for the study of a combined zone assembling partial oxidation and gasification. Adnan and Hussain[31] studied three different microalgae species gasification using the Gibbs free energy minimization approach. In their model using Aspen Plus, they focused on the combined gasification of biomass and tar to analyze the performance of the process. A similar study was performed by Zhai et al.[32] In their work, they investigated the effect of gasification temperature and steam amount on the carbon conversion rate and product gas properties.

From the above literature review, the importance of modeling biomass gasification using Aspen Plus has been highlighted. In addition, it has been shown that modeling the overall process could be enhanced by considering tar treatment. Therefore, the use of Aspen Plus is a reliable methodology that considers several specific aspects of the process founded on chemical reaction rates, hydrodynamics properties, and empirical correlations.

In the present study, a parametric study was performed to discuss the syngas composition and tar concentration, considering four compounds: toluene, phenol, benzene, and naphthalene. The main novelties of this work consist of refining previous studies,[33,34] allowing for enhanced predictions related to tar treatment modeling. In addition to the gas composition, the lower heating value and the cold gas efficiency were also investigated.

PROCESS MODELING

Process Description. The gasifier studied in this paper is based on uncoupling different parts of the process into three linked zones: biomass pyrolysis; subsequently, combustion of volatiles; and finally, char reduction, which occurs in a bubbling fluidized bed.[33] Pyrolysis occurs mainly between 500 and 600 °C, producing char particles, pyrolysis gas, and tar. Non-

https://doi.org/10.1021/acsomega.2c04492
ACS Omega 2022, 7, 33518−33529

Table 1. Chemical Reactions[35,36]

reaction	equation
1	$C + CO_2 \rightarrow 2\ CO$
2	$C + H_2O \rightarrow CO + H_2$
3	$C + 2\ H_2 \rightarrow CH_4$
4	$CO + H_2O \rightarrow CO_2 + H_2$
5	$CO_2 + H_2 \rightarrow CO + H_2O$
6	$CH_4 + H_2O \rightarrow CO + 3\ H_2$
7	$H_2 + 0.5\ O_2 \rightarrow H_2O$
8	$CO + 0.5\ O_2 \rightarrow CO_2$
9	$CH_4 + 2\ O_2 \rightarrow CO_2 + 2\ H_2O$
10	$C_6H_6O + 4\ O_2 \rightarrow 6\ CO + 3\ H_2O$
11	$C_6H_6O + 3\ H_2O \rightarrow 2\ CO + CO_2 + 2.95\ CH_4 + 0.05\ C + 0.1\ H_2$
12	$C_6H_6O \rightarrow CO + 0.75\ H_2 + 0.1\ CH_4 + 0.15\ C_6H_6 + 0.4\ C_{10}H_8$
13	$C_7H_8 + 3.5\ O_2 \rightarrow 7\ CO + 4\ H_2$
14	$2\ C_7H_8 + 21\ H_2O \rightarrow 7CO_2 + 29\ H_2 + 7\ CO$
15	$C_7H_8 + H_2 \rightarrow CH_4 + C_6H_6$
16	$C_6H_6 + 4.5\ O_2 \rightarrow 6\ CO + CO_2 + 3\ H_2O$
17	$C_6H_6 + 2\ H_2O \rightarrow 1.5\ C + 2.5\ CH_4 + 2\ CO$
18	$C_{10}H_8 \rightarrow 7,38\ C + 2.5\ C_6H_6 + 0,97\ CH_4 + 2.235\ H_2$

condensable gas and tar are reacted with oxygen present in the combustion zone. The gas issued from this zone with a large amount of heat is produced and served as the fluidizing medium. It is carried through a gas distributor to the fluidized bed of char particles in the reduction zone. A hot combustible gas is then generated. It is used to convey necessary heat for the pyrolyzer. Hence, instead of burning char, a portion of pyrolysis gas will be burnt. This operation method is different from what is expected from classical gasifiers, such as the dual fluidized-bed reactor (DFBG). Consequently, hot gases embody the gasification agent instead of using an additional preheated one. Table 1 displays several chemical reactions, homogeneous and heterogeneous, occurring during the gasification processes.[35,36] They present combustion and gasification reactions that take place in the combustion and gasification zones of the present gasifier. Chemical reaction rates are presented in Table 2.

A thermodynamic model to simulate Prosopis Juliflora gasification in a multistage reactor was developed in this study based on the approach of thermodynamic equilibrium using Aspen Plus. It has been established based on principles of mass, energy, and chemical balance. Thermodynamic equilibrium calculations are based on the Gibbs free energy minimization, presented by the RGIBBS block in Aspen Plus, as shown in the flowsheet of the studied model in Figure 1.

When it comes to biomass gasification modeling, the devolatilization process can be supposed to be instantaneous.[13] CO, CO_2, H_2, H_2O, CH_4, and tar compounds represent the main volatiles. The tar composition was specified corresponding to chemical composition, solubility, and condensability.[10,37,38] According to Abdelouahed et al.,[14] we can lump 10 tar species (benzene, phenol, cresols, toluene, o-xylene, indene, naphthalene, 1 + 2-methylnaphthalene, acenaphthylene, and phenanthrene) into four compounds: toluene, phenol, benzene, and naphthalene, as displayed in Table 3. This method can help in making the model less complicated.

Table 2. Chemical Reaction Rates[35,36]

reaction	reaction rates
1	$3.42\ T.\ \exp(-13 \times 10^3/R.\ T)[CO_2]$
2	$3.42\ T.\ \exp(-13 \times 10^3/R.\ T)[H_2O]$
3	$0.00342\ T.\ \exp(-13 \times 10^3/R.\ T)[H_2]$
4	$7.68 \times 10^{10}\ \exp(-3.046\ \times 10^5/R.\ T)[CO]^{0.5}[H_2O]$
5	$6.4 \times 10^9\ \exp(-3.264 \times 10^5/R.\ T)[H_2]^{0.5}[CO_2]$
6	$3 \times 10^5\ \exp(-1.25 \times 10^5/R.\ T)[CH_4][H_2O]$
7	$1.63 \times 10^{11}\ T^{-1.5}\ \exp(-2.85\ \times 10^4/R.\ T)[O_2][H_2]^{1.5}$
8	$5.62 \times 10^{12}\ \exp(-1.33 \times 10^5/R.\ T)[O_2]^{0.5}[CO]$
9	$3.552 \times 10^{11}\ \exp(-1.30529 \times 10^5/R.\ T)[O_2][CH_4]$
10	$2.4 \times 10^{11}\ \exp(-1.2552 \times 10^5/R.\ T)[C_6H_6O]^{0.1}[O_2]^{1.85}$
11	$10^8\ \exp(-10^5/R.\ T)[C_6H_6O]$
12	$10^7\ \exp(-10^5/R.\ T)[C_6H_6O]$
13	$1.3 \times 10^{11}\ T^{-1.5}\ \exp(-1.256 \times 10^5/R.\ T)[C_7H_8][O_2]^{0.5}$
14	$2.323 \times 10^5\ \exp(-3.56 \times 10^5/R.\ T)[C_7H_8]$
15	$3.3 \times 10^5\ T^{-1.5}\ \exp(-2.47 \times 10^5/R.\ T)[C_7H_8][H_2]^{0.5}$
16	$3.8 \times 10^7\ \exp(-5.545 \times 10^3/R.\ T)[C_6H_6][O_2]$
17	$3.39 \times 10^{16}\ \exp(-4.43 \times 10^5/R.\ T)[C_6H_6]^{1.3}[H_2O]^{0.2}[H_2]^{0.4}$
18	$3.39 \times 10^{14}\ \exp(-3.5 \times 10^5/R.\ T)[C_{10}H_8]^{1.6}[H_2O]^{0.2}[H_2]^{0.5}$

According to Chandrasekaran et al.,[39] Prosopis Juliflora proximate analysis and LHV are displayed in Table 4. In their study, they investigated the pyrolysis products: gas (CO, H_2, CO_2, and CH_4), char, and bio-oil. Neves et al.[17] mentioned that generally bio-oil refers to the entire liquid fraction, which includes organic compounds, i.e., tar, and moisture. As

https://doi.org/10.1021/acsomega.2c04492
ACS Omega 2022, 7, 33518−33529

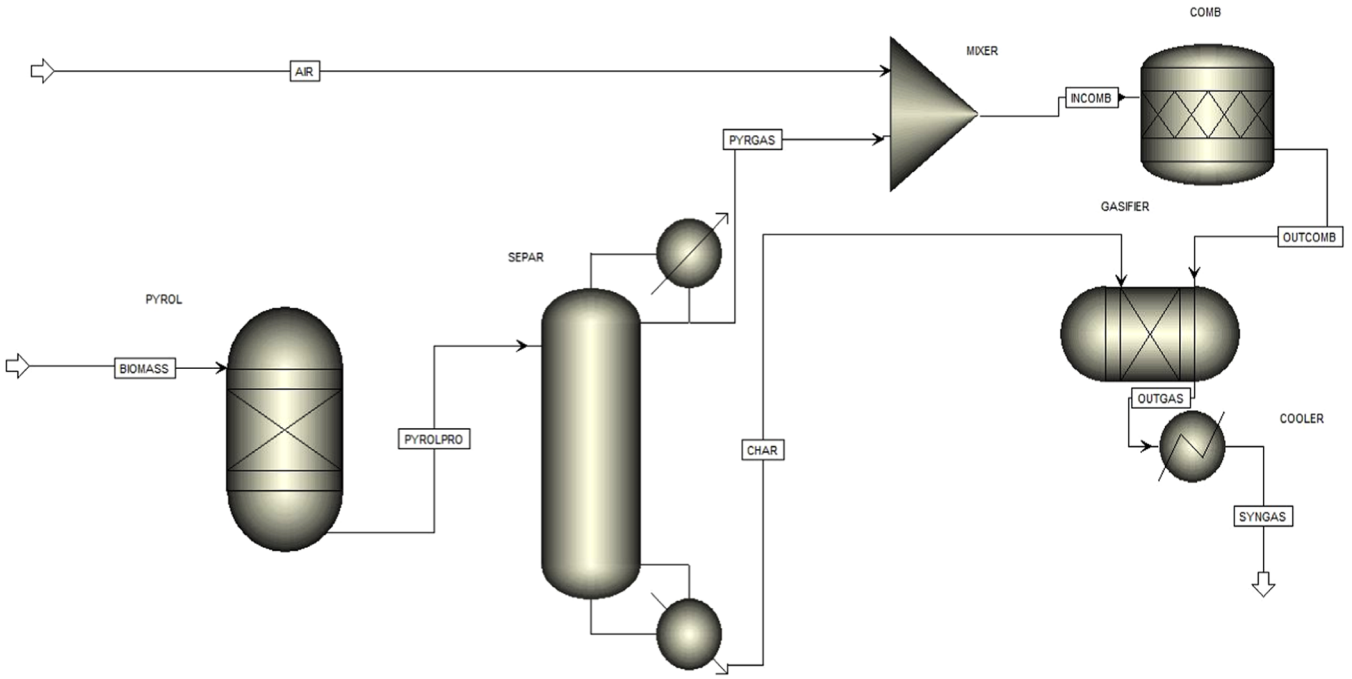

Figure 1. Model flowsheet.

Table 3. Lumped Species[14]

benzene	benzene
phenol	phenol and cresols
toluene	toluene, indene, and xylene
naphthalene	naphthalene, 1+2-methylnaphthalene, acenaphthylene, and phenanthrene

Table 4. Prosopis Juliflora Characteristics[39]

biomass particle size (mm)	0.2−0.5	0.5−1	1−2
volatile matter	77.5	76.2	76.9
ash content	3.7	4.1	3.9
fixed carbon	18.8	19.7	19.2
LHV (MJ/kg)	17.62	18.31	17.94

Chandrasekaran et al.[39] investigated the moisture content of the bio-oil produced, the tar yield could be concluded.

Table 5 displays six block types used in the Aspen Plus flowsheet. Pyrolysis gas and air are first mixed in a mixing block (MIXER). They are then conveyed to an RSTOIC block representing the combustion zone to model the oxidation reactions. Oxidized gas is then introduced to the RGIBBS reactor; it is mixed with char there to generate the product gas. The last block is the cooler, where the product gas is cooled to be generated at normal temperature and pressure. Data from Tables 1 and 2 are used in process modeling, in both RSTOIC and RGIBBS blocks. According to Mutlu and Zeng,[40] combustion in gasification processes is generally modeled in the RSTOIC block. It is used when the molar conversion and reaction stoichiometry are acknowledged for all of the occurring reactions. They can be modeled simultaneously or sequentially. Besides, product selectivity and reaction heat calculations can be done in this reactor. The block must have one or more feed streams; in our case, it is a mixture of air and pyrolysis gas, and one output stream.

Assuming the equilibrium approach, the RGIBBS block can be found and exploited from the Aspen Plus library. It is based on the minimization of the Gibbs free energy at equilibrium. It can be used to calculate the phase and chemical equilibrium

Table 5. Aspen Plus Blocks Used

Aspen Plus block type	Scheme	Description
RYIELD		Decomposition of biomass by specifying yields of the reaction of each component
SEPAR		Separates pyrolysis gas from solid particles of char
MIXER		Mixer, to combine pyrolysis gas and air streams into one stream
RSTOIC		Stoichiometric reactor to simulate combustion
RGIBBS		Gibbs free-energy reactor to simulate gasification
HEATER		Cooler, to have a syngas at normal temperature and pressure

https://doi.org/10.1021/acsomega.2c04492
ACS Omega 2022, 7, 33518−33529

Table 6. Mass Fraction of Different Pyrolysis Products Considered[39]

	T_p = 600 °C, d = 0.2−0.5 mm	T_p = 500 °C, d = 0.2−0.5 mm	T_p = 500 °C, d = 0.5−1 mm	T_p = 500 °C, d = 1−2 mm
solid	0.210	0.237	0.254	0.262
liquid	0.336	0.352	0.368	0.383
gas	0.454	0.411	0.378	0.355
		Gas and Tar Fraction Inlets		
CO	0.218	0.228	0.194	0.174
CO_2	0.161	0.191	0.220	0.226
H_2	0.095	0.058	0.041	0.037
CH_4	0.101	0.063	0.051	0.045
H_2O	0.225	0.243	0.269	0.278
benzene (C_6H_6)	0.076	0.082	0.085	0.091
phenol (C_6H_6O)	0.022	0.024	0.025	0.027
toluene (C_7H_8)	0.057	0.061	0.063	0.068
naphthalene ($C_{10}H_8$)	0.046	0.050	0.051	0.055

Table 7. Equivalence Ratio

air-to-biomass ratio	0.2	0.3	0.4	0.5	0.6	0.7	0.8	0.9	1	1.1	1.2
equivalence ratio	0.03	0.04	0.05	0.07	0.08	0.09	0.11	0.12	0.13	0.15	0.16

Table 8. Comparison of the Present Model Results with the Measured Data of Campoy et al.[41] and Beheshti et al.[13] (Adapted with Permission from ref 41. Copyright 2009 Elsevier Ltd. and ref 13. Copyright 2015 Elsevier Ltd.)

	OE = 40; ER = 0.32; S/B = 0.10					OE = 35; ER = 0.32; S/B = 0.31				
	syngas composition (vol/vol %, dry, N_2 free)				tar	syngas composition (vol/vol %, dry, N_2 free)				tar
	CO	H_2	CO_2	CH_4		CO	H_2	CO_2	CH_4	
present work	42.96	23.42	24.3	9.32	1.669	39.68	31.5	21.24	7.58	4.93
Campoy et al.[41] (experimental results)	39.60	26.50	23.40	10.5		36.10	33.90	19.00	11.00	
Beheshti et al.[13] (numerical results)	41.11	24.10	21.18	13.61	1.48	38.85	30.84	17.64	12.67	4.45

where reactions and inert components can be defined for the system.

To evaluate the system performance, cold gas efficiency CGE is considered. It can be calculated by eq 1, where LHV_{gas} and LHV_{fuel} are lower heating values of the producer gas (MJ/m^3) and fuel (MJ/kg), respectively. V_{gas} and m_{fuel} are the volumetric flow rate of the producer gas (Nm^3/s) and the mass flow rate of the fuel (kg/s), respectively.

The lower heating value of the product gas LHV_{gas} can be estimated by eq 2.[16]

$$CGE = \frac{LHV_{gas} V_{gas}}{LHV_{fuel} m_{fuel}} \quad (1)$$

$$LHV_{gas} = 12.64X_{CO} + 10.8X_{H_2} + 35.8X_{CH_4} [MJ/Nm^3] \quad (2)$$

where X_i is the mole fraction of the species i in the product gas.

Gas species (O_2, N_2, H_2, CO, CO_2, H_2O, and CH_4), char (containing 100% carbon), and tar are considered conventional components. The Peng−Robinson equation of state, allowing estimating all of the thermophysical properties in the stationary state, is selected. The present model assumed that the process is steady state, chemical reactions are at equilibrium, and combustion and gasification blocks are isothermal. Furthermore, the blocks used in this Aspen Plus model are implicitly considered zero-dimensional and characterized by perfect mixing and uniform temperature.

The biomass Prosopis Juliflora mass flow rate is 10 kg/h. Referring to Chandrasekaran's analysis,[39] pyrolysis products (gas, solid char, and liquid), displayed in Table 6 with specified mass fractions, generated from a fixed-bed pyrolyzer are considered as the inputs of combustion and gasification zones in our model. It is worth noting that the feedstock considered in this model is dry and ash-free. Two different pyrolysis temperatures Tp (600 °C and 500 °C) and three different ranges of particle sizes (0.2−0.5, 0.5−1, and 1−2 mm) were considered. The gasification atmospheric reactor is assumed isothermal between 800 °C and 1000 °C, and the airflow rate varied between 2 and 12 kg/h at 25 °C. The equivalence ratio (ER), defined as the mass ratio between the total and the stoichiometric amount of air fed in the reactor, is therefore varied between 0.03 and 0.16, as shown in Table 7.

In the following subsections, a parametric study of the effect of the air-to-biomass ratio and the gasification temperature is presented. Both combustion and gasification zones are considered in this study. Pyrolysis yields: char, pyrolysis gas, and tar were used as inputs in the subsequent steps. The main studied output variables were the syngas composition, its lower heating value, and the cold gas efficiency of the reactor. The presence of tar in the pyrolysis gas is considered in simulations. Naphthalene, toluene, phenol, and benzene are the principal tar components.

RESULTS AND DISCUSSIONS

Validation. The model was validated to verify its accuracy by comparing its findings to existing data from the literature. The present biomass gasification model results, as shown in Table 8, have been compared to numerical and experimental data of Beheshti et al.[13] and Campoy et al.,[41] respectively. They both studied the composition of the syngas produced by wood pellet gasification in a bubbling fluidized-bed reactor. Enriched air with oxygen and steam was considered as the gasification agent.

https://doi.org/10.1021/acsomega.2c04492
ACS Omega 2022, 7, 33518−33529

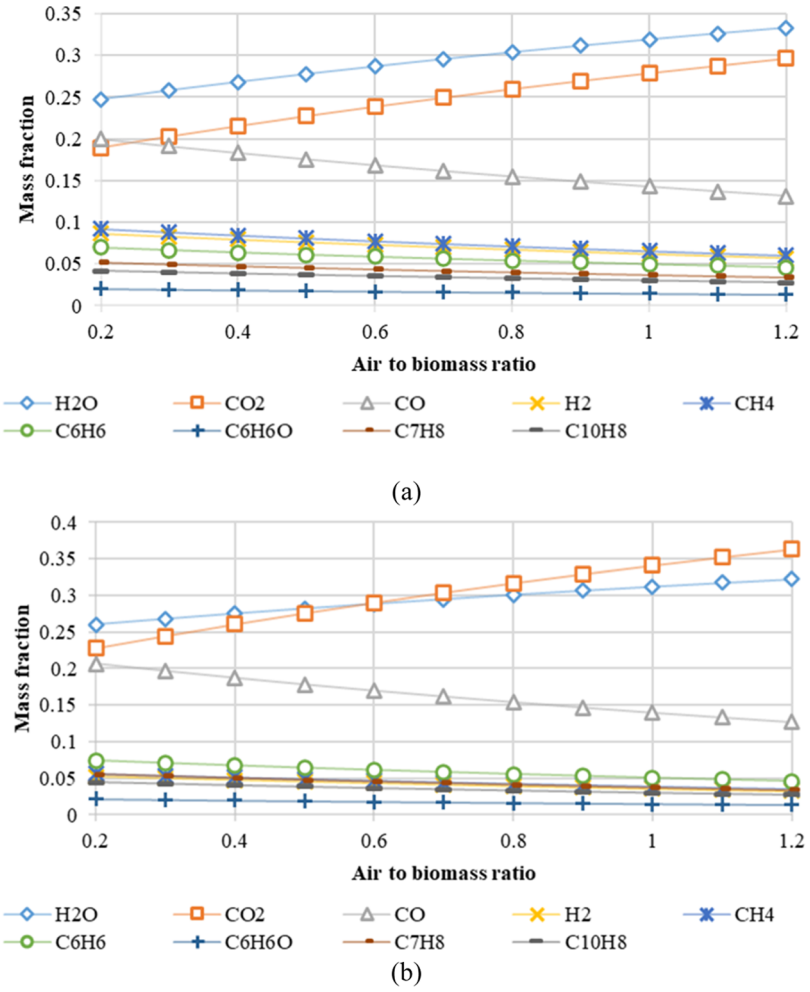

Figure 2. Effect of the air-to-biomass ratio on the gas composition, N_2-free, issued from the combustion zone for particle sizes between 0.2 and 0.5 mm and two pyrolysis temperatures (a) T_p = 600 °C and (b) T_p = 500 °C.

Comparison was made for different operation conditions: (1) oxygen percentage of the enriched air (OE) = 40; equivalence ratio (ER) = 0.32; steam-to-biomass ratio (S/B) = 0.10; and (2) OE = 35; ER = 0.32; and S/B = 0.31. Similar results were obtained in the numerical simulations of the present model compared to the existing experimental and numerical findings, according to Table 8.

Parametric Study. *Combustion Zone.* Figure 2 shows the effect of the air-to-biomass ratio on the gas composition issued from the combustion zone. Results shown in this section are N_2-free. The Prosopis Juliflora particle size range considered is between 0.2 and 0.5 mm as it is the range that showed optimal products. As expected, CO_2 and H_2O are the governing products in the presence of the other compounds. Both CO_2 and H_2O showed an increasing tendency while increasing the air-to-biomass ratio, while all of the other compounds showed a decreasing tendency. The mass fraction of H_2O is almost the same, with values from around 0.25 to 0.33 for air-to-biomass ratios of 0.2−1.2, respectively, for both pyrolysis temperatures tested. However, the mass fraction of CO2 increased more rapidly for T_p = 500 °C in the range of 0.22−0.36 for air-to-biomass ratios of 0.2−1.2, respectively. This could be related to the mass fraction of CO, which decreased faster for T_p = 500 °C. It may be due also to the concentration of CO in the pyrolysis products, which was more important for T_p = 500 °C compared to T_p = 600 °C. With the increase in the air/biomass ratio, the amount of oxygen supplied in the combustor intensifies. The gas components produced during the process of pyrolysis burn inside the combustor and produce more heat. As a result, the temperature increases in the combustion reactor and leads to enhancing the gasification reactions occurring inside the gasifier. On the other hand, the concentration of the product gas will be diluted significantly.

Tar species were also affected by the air-to-biomass ratio and showed decreasing tendencies. Figure 3 displays the total tar mass fraction issued from the combustion zone against the air-

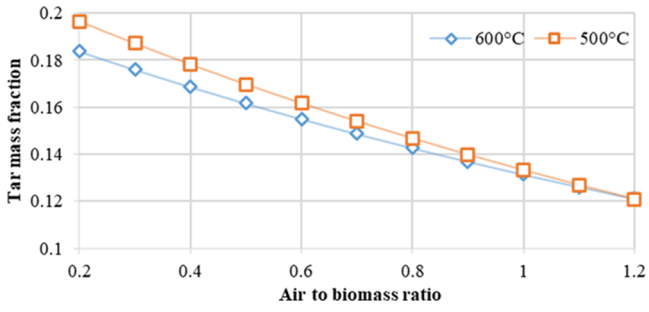

Figure 3. Effect of the air-to-biomass ratio on the tar mass fraction, N_2-free, issued from the combustion zone for particle sizes between 0.2 and 0.5 mm and two pyrolysis temperatures: T_p = 600 °C and T_p = 500 °C.

https://doi.org/10.1021/acsomega.2c04492
ACS Omega 2022, 7, 33518−33529

to-biomass ratio for both pyrolysis temperatures studied. For small air-to-biomass ratios, tar issued from pyrolysis of T_p = 500 °C shows slightly higher values after combustion than that issued from pyrolysis of 600 °C. In fact, originally tar yields from pyrolysis at a temperature of 500 °C are greater than those from 600 °C. By increasing the ER value, a reduction in tar content caused by the oxidation reactions of tar species (Reactions 10, 13, and 16) is observed. Beheshti et al.[13] stated that it is due to a significant increase in the thermal cracking of tar.

Gasification Zone. According to the gasification system studied in this paper, oxidized pyrolysis gas, issued from the combustion chamber, is used as the fluidizing medium of the gasification chamber, where char particles are reduced in a temperature greater than 800 °C.

In this section, the product gas generated from the gasification zone is analyzed. It is about a parametric study to inspect the effect of the gasification temperature, air-to-biomass ratio, and biomass characteristics on the gas composition and system efficiency.

Figure 4 shows the mass fraction of produced syngas compounds: CO, H_2, and CH_4, for air-to-biomass ratios from 0.2 to 1.2 and for gasification temperature from 800 to 1000 °C. In all cases, increasing the airflow rate had a common effect on diluting the gas produced. CO mass fractions slightly increased with the increase in temperature and decreased with the increase of the air-to-biomass ratio. In fact, for T = 800 °C, the CO mass fraction varied from 0.58 to 0.48 for an air/biomass ratio range of 0.2−1.2, respectively, and from 0.48 to 0.5 from 800 to 1000 °C for an air/biomass ratio of 1.2. Consequently, the amount of air introduced to the system, whether by focusing on the air/biomass ratio or the equivalence ratio ER, contributes to a decrease in the CO mass fraction while raising the CO_2. This could be due to the combined effect of the combustion reaction producing CO_2 (Reactions 8, 9, and 16) and the Boudouard reaction (Reaction 1). As a result, for lower ER values, Reaction 1 tends to add more CO to the system at the expense of CO_2, but at higher ER values, Reaction 8 converts more CO into CO_2. Jayathilake and Rudra[42] also reported that ER could have a combined effect on CO and CO_2 production. It can be observed that higher temperatures contributed to higher hydrogen contents in the syngas. Similar findings were reported in the literature.[43] The higher the temperature, the more the energy available for the endothermic reaction of hydrogen generation, increasing the hydrogen content of the syngas.

A different behavior could be seen in H_2 mass fractions where less air-to-biomass ratio values showed an important dependence on the gasification temperature. In fact, for an air-to-biomass ratio of 0.2, the H_2 mass fraction increased from 0.042 to 0.058 from 800 to 1000 °C, respectively. However, it is still insignificant compared to the CO mass fraction. This is due to the presence of char in the gasifier as a main compound to be converted mainly into CO. Increasing both the gasification temperature and the air-to-biomass ratio had a negative effect on CH_4 mass fractions. The greater value, 0.25, was observed for T = 800 °C and an air-to-biomass ratio of 0.2.

Accordingly, Gagliano et al.[44] stated that with increasing ER, the concentration of CH_4 in the syngas decreases. These observations can be confirmed by the results displayed in Figure 5. It shows the mass yields of CO, H_2, and CH_4, for air-to-biomass ratios from 0.2 to 1.2, gasification temperatures from 800 to 1000 °C, and pyrolysis temperatures 600 and 500 °C. A considerable difference could be observed between results of T_p = 600 and 500 °C. The maximum values of mass yields from

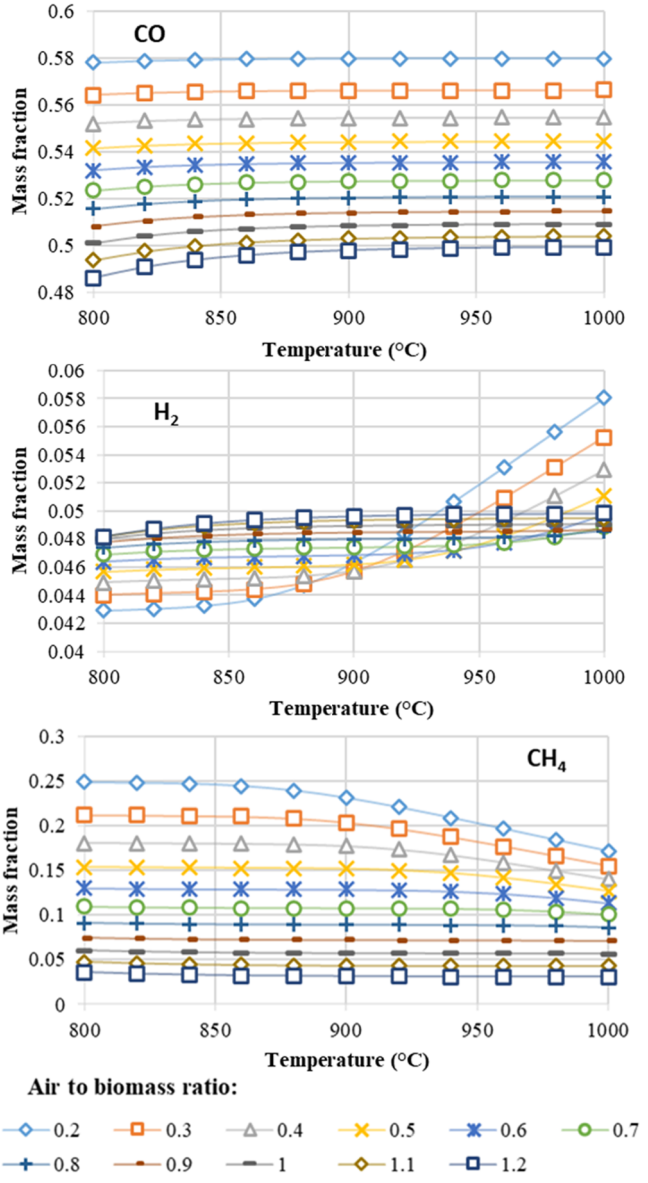

Figure 4. Effect of gasification temperature and air-to-biomass ratio on mass fractions of CO, H_2, and CH_4 produced from the gasification zone for particle sizes between 0.2 and 0.5 mm and pyrolysis temperature T_p = 600 °C.

Figure 5a are greater than those of Figure 5b. CO and H_2 mass yields were increased with the increase in temperature and air-to-biomass ratios and reached maxima of 11 kg/h and 1.1 kg/h, respectively, for T = 1000 °C, air-to-biomass ratio = 1.2, and T_p = 600 °C. The opposite behavior was observed on CH_4 mass yield. A maximum value of 3 kg/h was obtained when T = 800 °C was observed. The optimal conditions for CO and H_2 mass yields represent the minimum value for the CH_4 mass yield with 0.68 kg/h.

Tar Yield. The total tar mass fraction issued from the gasification zone was affected by the gasification temperature, air-to-biomass ratio, and pyrolysis temperatures, as shown in Figure 6. An increase in the air fed to the system led to a considerable decrease in the tar concentration, which reached almost zero for air-to-biomass ratios greater than 0.9. As discussed in 3.2.1, combustion of pyrolysis products of T_p = 500 °C generated more tar. The same behavior could be seen in the

https://doi.org/10.1021/acsomega.2c04492
ACS Omega 2022, 7, 33518−33529

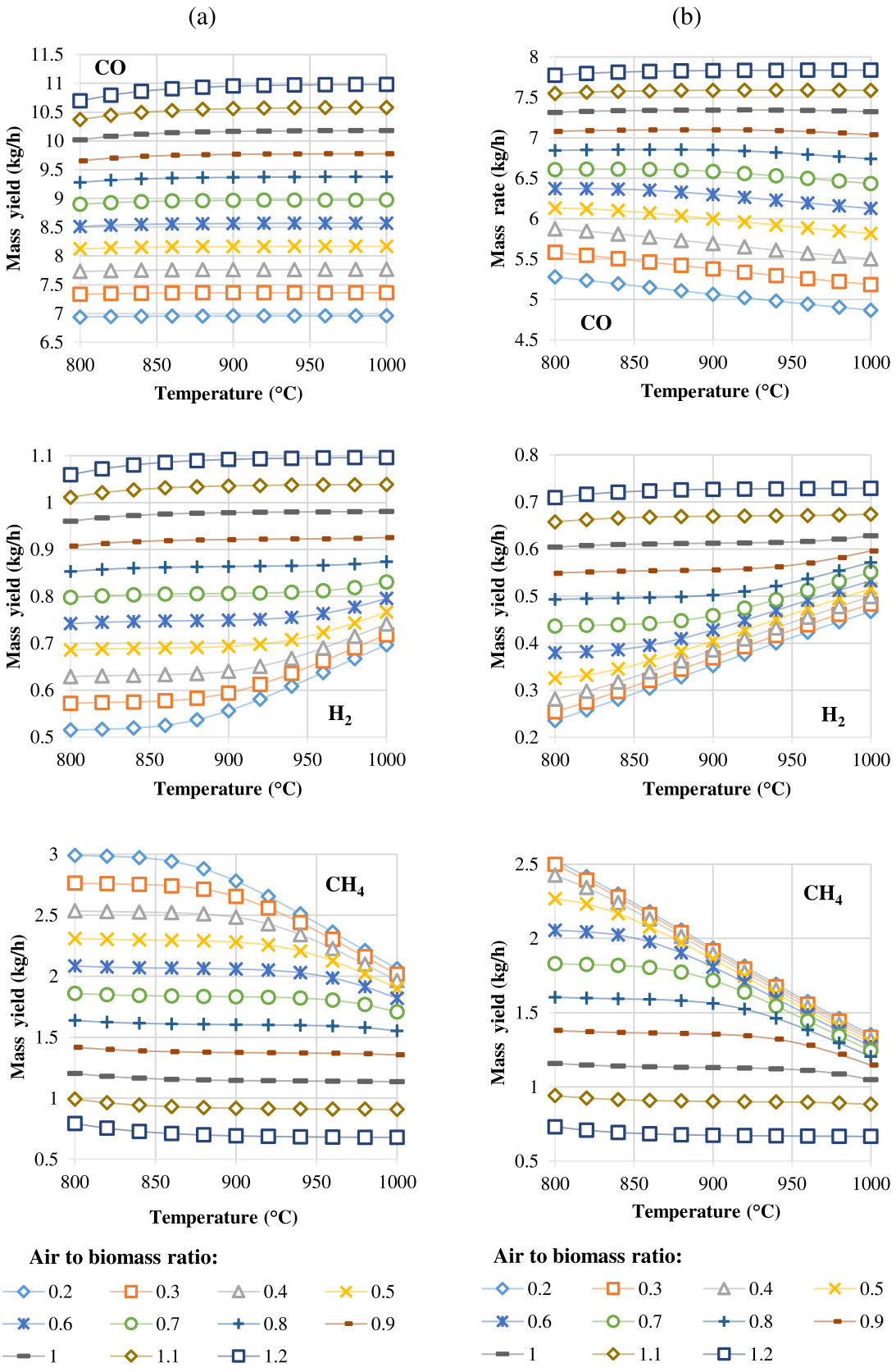

Figure 5. Effect of gasification temperature and air-to-biomass ratio on mass yields of CO, H_2, and CH_4 produced from the gasification zone for particle sizes between 0.2 and 0.5 mm and two pyrolysis temperatures: (a) T_p = 600 °C and (b) T_p = 500 °C.

gasification zone where mass fraction values in Figure 6b are higher than those in Figure 6a. Regarding the temperature effect, it can be seen that thermal cracking of tar should be functioning with an adequate equivalence ratio. It should be greater than 0.09 (air-to-biomass ratio of 0.7). Furthermore, according to Chen et al.'s experimental studies,[45] the influence of air on tar

https://doi.org/10.1021/acsomega.2c04492
ACS Omega 2022, 7, 33518−33529

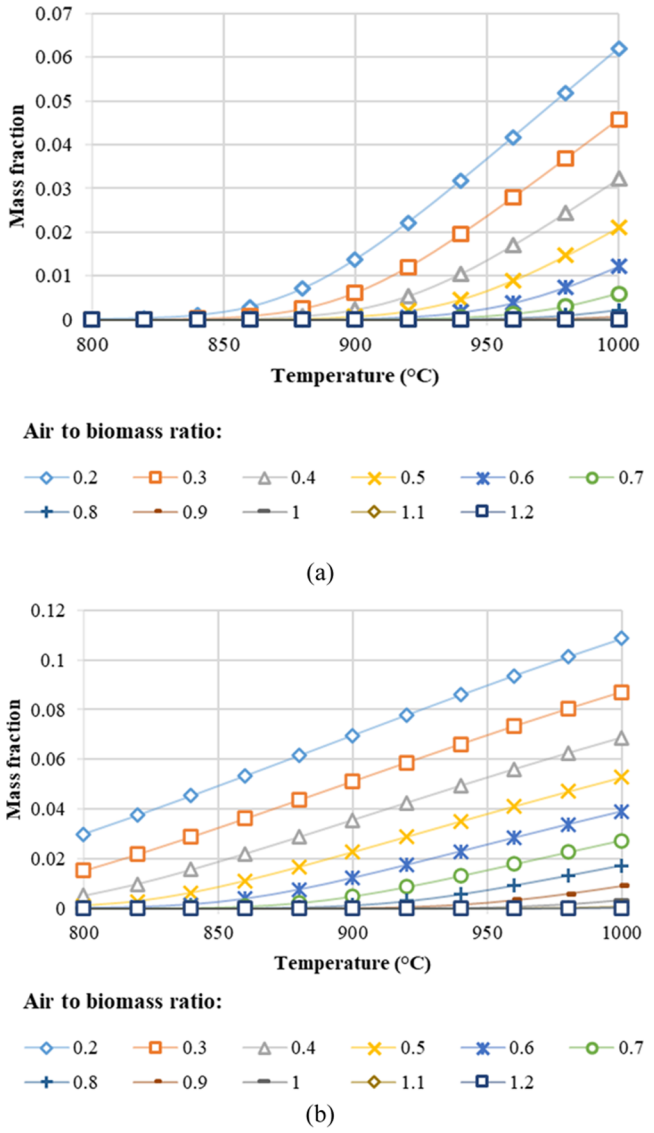

Figure 6. Effect of gasification temperature and air-to-biomass ratio on the mass fraction of the total tar produced from the gasification zone for particle sizes between 0.2 and 0.5 mm and two pyrolysis temperatures: (a) T_p = 600 °C and (b) T_p = 500 °C.

has been revealed. They stated that the addition of air resulted in a reduction in the tar concentration in the producer gas. Striūgas et al.[46] reported that reducing the ER to 0.02 generated more tar content, and the ideal air equivalence ratio, which corresponded to the most reduced tar content, was found to be ER = 0.5. However, they noted that based on the gas composition (CO, H_2, and CH_4 contents) and tar content together, the optimum air equivalence ratio was found to be 0.07. Therefore, an arrangement between these two points must be achieved. It could be determined by calculating and analyzing the LHV of the product gas and the CGE, in addition to the total tar content.

Figure 7 presents the effect of the pyrolysis temperature and biomass particle size on the total amount of tar generated from the gasification process. It shows that tar is less produced with a pyrolysis temperature of 600 °C. Particle size also affected the tar yield as better results (with less tar generated) were observed with a smaller particle size. Increasing the air fed to the system contributed to an increase in H_2O as a combustion product (Reactions 7, 9, and 10) and contributed then to decreasing the tar amount in the syngas (Reactions 11, 14, and 17). Therefore, for an air-to-biomass ratio of 1.2, the tar amount is almost 0 kg/h.

Figure 8 displays the effect of gasification temperature and the air-to-biomass ratio on the LHV and CGE of the gasification process studied. They are calculated using eqs 1 and 2, respectively. LHV reached a maximum value of 16.1 MJ/Nm3 with a gasification temperature of 800 °C and an air-to-biomass ratio of 0.2. This is due to the high concentration of CO, H_2, and CH_4 in the product gas generated in these operating conditions. By increasing the value of the air-to-biomass ratio, the percentages of the gaseous species that contribute to the calculation of the LHV decrease to reach a minimum value of 9.3 MJ/Nm^3. They are seen at a fixed value for the different temperatures studied. For every temperature value, the CGE increased by increasing the air-to-biomass ratio to 1.2 to reach a maximum CGE of 69%. Decreasing tendencies of CGE were observed while increasing the gasification temperature, which could be due to the decrease in the CH_4 amount in the syngas. Similar findings were reported by Campoy et al.[41] and Beheshti et al.[13]

CONCLUSIONS

In this study, Prosopis Juliflora gasification was developed in an atmospheric fluidized-bed gasifier using an Aspen Plus Model. The considered system was a multistage system that modeled pyrolysis, combustion, and reduction separately in different blocks. Numerical investigation was performed to study the gas

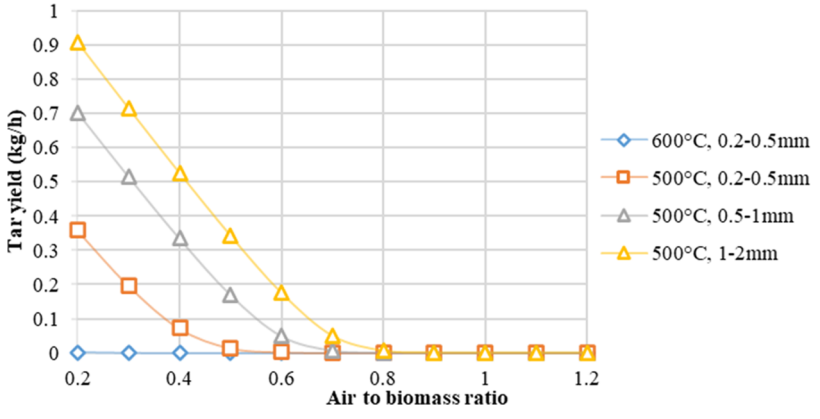

Figure 7. Effect of pyrolysis temperature and Prosopis Juliflora particle size on the tar mass yield from gasification at 800 °C.

https://doi.org/10.1021/acsomega.2c04492
ACS Omega 2022, 7, 33518−33529

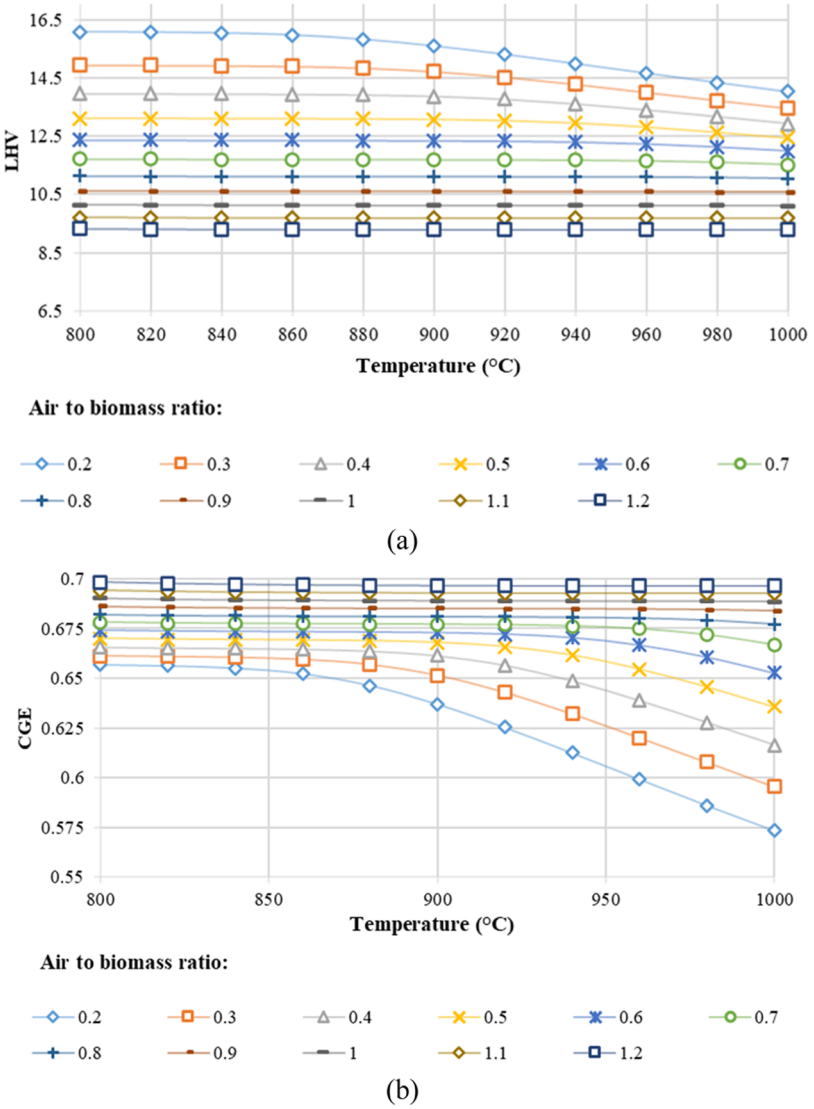

Figure 8. Effect of gasification temperature and the air-to-biomass ratio on (a) LHV and (b) CGE.

composition and tar yield produced for different air mass flow rates and temperature values. In this work, the biomass devolatilization was supposed instantaneous and the produced gas and char resulting from pyrolysis were used as entries of the combustion and reduction zones, respectively. Results revealed that CO was the principal component, and its mass fraction was slightly increased with the increase in temperature from 800 to 1000 °C and decreased with the increase in the air-to-biomass ratio from 0.2 to 1.2, and it increased significantly with the increase of the gasifier temperature. It shows that tar production is reduced with a pyrolysis temperature of 600 °C. Particle size also affects the tar yield; a small particle size produced less amount of tar. Results showed that despite the positive effect of the gasification temperature increase on the gas species CO and H_2, there was a negative consequence on the tar species. CGE was maximized to 69% with almost zero tar amount produced for a gasification temperature of 800 °C and an air-to-biomass ratio of 1.2.

AUTHOR INFORMATION

Corresponding Author

Walid Hassen − *Laboratory of Metrology and Energy Systems, Monastir, University of Monastir, 5000 Monastir, Tunisia;* orcid.org/0000-0002-6779-2335; Email: hassen.walid@gmail.com

Authors

Maryem Dhrioua − *Laboratory of Metrology and Energy Systems, Monastir, University of Monastir, 5000 Monastir, Tunisia*

Kaouther Ghachem − *Department of Industrial Engineering and Systems, College of Engineering, Princess Nourah bint Abdulrahman University, Riyadh 11671, Saudi Arabia*

Ahmed Ghazy − *Mechanical Engineering Department, College of Engineering, Jouf University, Sakaka 72388 Aljouf, Saudi Arabia*

Lioua Kolsi − *Mechanical Engineering Department, College of Engineering, University of Ha'il, 81451 Ha'il City, Saudi Arabia*

Mohamed Naceur Borjini − *Laboratory of Metrology and Energy Systems, Monastir, University of Monastir, 5000 Monastir, Tunisia*

https://doi.org/10.1021/acsomega.2c04492
ACS Omega 2022, 7, 33518−33529

Complete contact information is available at:
https://pubs.acs.org/10.1021/acsomega.2c04492

Notes

The authors declare no competing financial interest.

■ ACKNOWLEDGMENTS

The authors acknowledge Princess Nourah bint Abdulrahman University Researchers Supporting Project number (PNURSP2022R41), Princess Nourah bint Abdulrahman University, Riyadh, Saudi Arabia. This research was part of an international project that is undertaken with the support of the Tunisian ministry of higher education and research and the Department of Science and Technology of the Government of India in the framework of the Tunisian-Indian cooperation in scientific research and technology.

■ REFERENCES

(1) Basu, P.*Biomass Gasification and Pyrolysis: Practical Design and Theory*; Academic Press, 2010.
(2) Henriksen, U.; Ahrenfeldt, J.; Jensen, T. K.; Gøbel, B.; Bentzen, J. D.; Hindsgaul, C.; Sørensen, L. H. The Design, Construction and Operation of a 75kW Two-Stage Gasifier. *Energy* **2006**, *31*, 1542−1553.
(3) Antonopoulos, I.-S.; Karagiannidis, A.; Elefsiniotis, L.; Perkoulidis, G.; Gkouletsos, A. Development of an Innovative 3-Stage Steady-Bed Gasifier for Municipal Solid Waste and Biomass. *Fuel Process. Technol.* **2011**, *92*, 2389−2396.
(4) Nilsson, S.; Gómez-Barea, A.; Cano, D. F. Gasification Reactivity of Char from Dried Sewage Sludge in a Fluidized Bed. *Fuel* **2012**, *92*, 346−353.
(5) Gómez-Barea, A.; Leckner, B.; Villanueva Perales, A.; Nilsson, S.; Fuentes Cano, D. Improving the Performance of Fluidized Bed Biomass/Waste Gasifiers for Distributed Electricity: A New Three-Stage Gasification System. *Appl. Therm. Eng.* **2013**, *50*, 1453−1462.
(6) Heidenreich, S.; Foscolo, P. U. New Concepts in Biomass Gasification. *Prog. Energy Combust. Sci.* **2015**, *46*, 72−95.
(7) Choi, Y.-K.; Mun, T.-Y.; Cho, M.-H.; Kim, J.-S. Gasification of Dried Sewage Sludge in a Newly Developed Three-Stage Gasifier: Effect of Each Reactor Temperature on the Producer Gas Composition and Impurity Removal. *Energy* **2016**, *114*, 121−128.
(8) Choi, Y.-K.; Ko, J.-H.; Kim, J.-S. A New Type Three-Stage Gasification of Dried Sewage Sludge: Effects of Equivalence Ratio, Weight Ratio of Activated Carbon to Feed, and Feed Rate on Gas Composition and Tar, NH3, and H2S Removal and Results of Approximately 5 h Gasification. *Energy* **2017**, *118*, 139−146.
(9) Choi, Y.-K.; Ko, J.-H.; Kim, J.-S. Gasification of Dried Sewage Sludge Using an Innovative Three-Stage Gasifier: Clean and H2-Rich Gas Production Using Condensers as the Only Secondary Tar Removal Apparatus. *Fuel* **2018**, *216*, 810−817.
(10) Valderrama Rios, M. L.; González, A. M.; Lora, E. E. S.; Almazán del Olmo, O. A. Reduction of Tar Generated during Biomass Gasification: A Review. *Biomass Bioenergy* **2018**, *108*, 345−370.
(11) Loha, C.; Gu, S.; De Wilde, J.; Mahanta, P.; Chatterjee, P. K. Advances in Mathematical Modeling of Fluidized Bed Gasification. *Renewable Sustainable Energy Rev.* **2014**, *40*, 688−715.
(12) Esmaili, E.; Mahinpey, N.; Mostafavi, E. An Extensive Simulation of Coal Gasification in Bubbling Fluidized Bed: Integration of Hydrodynamics into Reaction Modelling. *Can. J. Chem. Eng.* **2014**, *92*, 1714−1724.
(13) Beheshti, S. M.; Ghassemi, H.; Shahsavan-Markadeh, R. Process Simulation of Biomass Gasification in a Bubbling Fluidized Bed Reactor. *Energy Convers. Manage.* **2015**, *94*, 345−352.
(14) Abdelouahed, L.; Authier, O.; Mauviel, G.; Corriou, J. P.; Verdier, G.; Dufour, A. Detailed Modeling of Biomass Gasification in Dual Fluidized Bed Reactors under Aspen Plus. *Energy Fuels* **2012**, *26*, 3840−3855.
(15) Pauls, J. H.; Mahinpey, N.; Mostafavi, E. Simulation of Air-Steam Gasification of Woody Biomass in a Bubbling Fluidized Bed Using Aspen Plus: A Comprehensive Model Including Pyrolysis, Hydrodynamics and Tar Production. *Biomass Bioenergy* **2016**, *95*, 157−166.
(16) Cheng, Y.; Thow, Z.; Wang, C.-H. Biomass Gasification with CO2 in a Fluidized Bed. *Powder Technol.* **2016**, *296*, 87−101.
(17) Neves, D.; Thunman, H.; Matos, A.; Tarelho, L.; Gómez-Barea, A. Characterization and Prediction of Biomass Pyrolysis Products. *Prog. Energy Combust. Sci.* **2011**, *37*, 611−630.
(18) Puig-Arnavat, M.; Bruno, J. C.; Coronas, A. Review and Analysis of Biomass Gasification Models. *Renewable Sustainable Energy Rev.* **2010**, *14*, 2841−2851.
(19) Adeyemi, I.; Janajreh, I. Modeling of the Entrained Flow Gasification: Kinetics-Based ASPEN Plus Model. *Renewable Energy* **2015**, *82*, 77−84.
(20) Doherty, W.; Reynolds, A.; Kennedy, D. The Effect of Air Preheating in a Biomass CFB Gasifier Using ASPEN Plus Simulation. *Biomass Bioenergy* **2009**, *33*, 1158−1167.
(21) Ramzan, N.; Ashraf, A.; Naveed, S.; Malik, A. Simulation of Hybrid Biomass Gasification Using Aspen plus: A Comparative Performance Analysis for Food, Municipal Solid and Poultry Waste. *Biomass Bioenergy* **2011**, *35*, 3962−3969.
(22) Niu, M.; Huang, Y.; Jin, B.; Wang, X. Simulation of Syngas Production from Municipal Solid Waste Gasification in a Bubbling Fluidized Bed Using Aspen Plus. *Ind. Eng. Chem. Res.* **2013**, *52*, 14768−14775.
(23) Mitta, N. R.; Ferrer-Nadal, S.; Lazovic, A. M.; Parales, J. F.; Velo, E.; Puigjaner, L.Modelling and Simulation of a Tyre Gasification Plant for Synthesis Gas Production. In *Computer Aided Chemical Engineering*, Marquardt, W.; Pantelides, C., Eds.; 16th European Symposium on Computer Aided Process Engineering and 9th International Symposium on Process Systems Engineering, Elsevier, 2006; Vol. *21*, pp 1771−1776.
(24) Renganathan, T.; Yadav, M. V.; Pushpavanam, S.; Voolapalli, R. K.; Cho, Y. S. CO2 Utilization for Gasification of Carbonaceous Feedstocks: A Thermodynamic Analysis. *Chem. Eng. Sci.* **2012**, *83*, 159−170.
(25) Ravikiran, A.; Renganathan, T.; Pushpavanam, S.; Voolapalli, R. K.; Cho, Y. S. Generalized Analysis of Gasifier Performance Using Equilibrium Modeling. *Ind. Eng. Chem. Res.* **2012**, *51*, 1601−1611.
(26) Adnan, M. A.; Susanto, H.; Binous, H.; Muraza, O.; Hossain, M. M. Feed Compositions and Gasification Potential of Several Biomasses Including a Microalgae: A Thermodynamic Modeling Approach. *Int. J. Hydrogen Energy* **2017**, *42*, 17009−17019.
(27) Su, Y.; Luo, Y.; Chen, Y.; Wu, W.; Zhang, Y. Experimental and Numerical Investigation of Tar Destruction under Partial Oxidation Environment. *Fuel Process. Technol.* **2011**, *92*, 1513−1524.
(28) Kaushal, P.; Tyagi, R. Advanced Simulation of Biomass Gasification in a Fluidized Bed Reactor Using ASPEN PLUS. *Renewable Energy* **2017**, *101*, 629−636.
(29) Liu, H.Biomass Fuels for Small and Micro Combined Heat and Power (CHP) Systems: Resources, Conversion and Applications. In *Small and Micro Combined Heat and Power (CHP) Systems*, Beith, R., Ed.; Woodhead Publishing Series in Energy; Woodhead Publishing, 2011; pp 88−122.
(30) Masmoudi, M. A.; Halouani, K.; Sahraoui, M. Comprehensive Experimental Investigation and Numerical Modeling of the Combined Partial Oxidation-Gasification Zone in a Pilot Downdraft Air-Blown Gasifier. *Energy Convers. Manage.* **2017**, *144*, 34−52.
(31) Adnan, M. A.; Hossain, M. M. Gasification Performance of Various Microalgae Biomass − A Thermodynamic Study by Considering Tar Formation Using Aspen Plus. *Energy Convers. Manage.* **2018**, *165*, 783−793.
(32) Zhai, M.; Guo, L.; Wang, Y.; Zhang, Y.; Dong, P.; Jin, H. Process Simulation of Staging Pyrolysis and Steam Gasification for Pine Sawdust. *Int. J. Hydrogen Energy* **2016**, *41*, 21926−21935.
(33) Dhrioua, M.; Hassen, W.; Kolsi, L.; Anbumalar, V.; Alsagri, A. S.; Borjini, M. N. Gas Distributor and Bed Material Effects in a Cold Flow

Model of a Novel Multi-Stage Biomass Gasifier. *Biomass Bioenergy* **2019**, *126*, 14−25.
(34) Dhrioua, M.; Hassen, W.; Kolsi, L.; Ghachem, K.; Maatki, C.; Borjini, M. N. Simulation of Prosopis Juliflora Air Gasification in Multistage Fluidized Process. *Processes* **2020**, *8*, 1655.
(35) Gerber, S.; Behrendt, F.; Oevermann, M. An Eulerian Modeling Approach of Wood Gasification in a Bubbling Fluidized Bed Reactor Using Char as Bed Material. *Fuel* **2010**, *89*, 2903−2917.
(36) Xie, J.; Zhong, W.; Jin, B.; Shao, Y.; Liu, H. Simulation on Gasification of Forestry Residues in Fluidized Beds by Eulerian−Lagrangian Approach. *Bioresour. Technol.* **2012**, *121*, 36−46.
(37) Anis, S.; Zainal, Z. A. Tar Reduction in Biomass Producer Gas via Mechanical, Catalytic and Thermal Methods: A Review. *Renewable Sustainable Energy Rev.* **2011**, *15*, 2355−2377.
(38) Ahmed, A. M. A.; Salmiaton, A.; Choong, T. S. Y.; Wan Azlina, W. A. K. G. Review of Kinetic and Equilibrium Concepts for Biomass Tar Modeling by Using Aspen Plus. *Renewable Sustainable Energy Rev.* **2015**, *52*, 1623−1644.
(39) Chandrasekaran, A.; Ramachandran, S.; Subbiah, S. Modeling, Experimental Validation and Optimization of Prosopis Juliflora Fuelwood Pyrolysis in Fixed-Bed Tubular Reactor. *Bioresour. Technol.* **2018**, *264*, 66−77.
(40) Mutlu, Ö. Ç.; Zeng, T. Challenges and Opportunities of Modeling Biomass Gasification in Aspen Plus: A Review. *Chem. Eng. Technol.* **2020**, *43*, 1674−1689.
(41) Campoy, M.; Gómez-Barea, A.; Vidal, F. B.; Ollero, P. Air−Steam Gasification of Biomass in a Fluidised Bed: Process Optimisation by Enriched Air. *Fuel Process. Technol.* **2009**, *90*, 677−685.
(42) Jayathilake, R.; Rudra, S. Numerical and Experimental Investigation of Equivalence Ratio (ER) and Feedstock Particle Size on Birchwood Gasification. *Energies* **2017**, *10*, 1232.
(43) Kumar, A.; Eskridge, K.; Jones, D. D.; Hanna, M. A. Steam−Air Fluidized Bed Gasification of Distillers Grains: Effects of Steam to Biomass Ratio, Equivalence Ratio and Gasification Temperature. *Bioresour. Technol.* **2009**, *100*, 2062−2068.
(44) Gagliano, A.; Nocera, F.; Bruno, M.; Cardillo, G. Development of an Equilibrium-Based Model of Gasification of Biomass by Aspen Plus. *Energy Procedia* **2017**, *111*, 1010−1019.
(45) Chen, Y.; Luo, Y.; Wu, W.; Su, Y.*Experimental Investigation on Tar Formation and Destruction in a Lab-Scale Two-Stage Reactor*; ACS Publications. https://pubs.acs.org/doi/pdf/10.1021/ef900623n (accessed July 15, 2022).
(46) Striūgas, N.; Zakarauskas, K.; Stravinskas, G.; Grigaitienė, V. Comparison of Steam Reforming and Partial Oxidation of Biomass Pyrolysis Tars over Activated Carbon Derived from Waste Tire. *Catal. Today* **2012**, *196*, 67−74.

https://doi.org/10.1021/acsomega.2c04492
ACS Omega 2022, 7, 33518−33529